Talanta 116 (2013) 1054–1059

Contents lists available at ScienceDirect

Talanta

journal homepage: www.elsevier.com/locate/talanta

One-step fabrication of bio-functionalized nanoporous gold/poly(3,4-ethylenedioxythiophene) hybrid electrodes for amperometric glucose sensing

Xinxin Xiao, Meng'en Wang, Hui Li, Pengchao Si *

Key Laboratory for Liquid-Solid Structural Evolution and Processing of Materials, Ministry of Education, School of Materials Science and Engineering, Shandong University, Jinan 250061, People's Republic of China

ARTICLE INFO

Article history:
Received 15 May 2013
Received in revised form
31 July 2013
Accepted 11 August 2013
Available online 17 August 2013

Keywords:
Nanoporous gold
Poly(3,4-ethylenedioxythiophene)
Glucose biosensor
Electropolymerization

ABSTRACT

We report a simple, one-step synthesis of hybrid film by electropolymerizing 3,4-ethylenedioxythiophene (EDOT) on nanoporous gold (NPG) for applications in amperometric glucose biosensors. The enzyme, glucose oxidase (GOx), is entrapped into poly(3,4-ethylenedioxythiophene) (PEDOT) matrix, simultaneously. Scanning electron microscope (SEM) and transmission electron microscopy (TEM) studies show the NPG preserve its original bicontinuous nanoporous structure and the PEDOT film grows uniformly with a thickness of ~10 nm. The modified electrodes have been investigated by cyclic voltammetry (CV) and single potential step chronoamperometry (SPSC). The influence of PEDOT film's thickness has been explored to optimize sensor behaviors. Mediated by p-benzoquinone (BQ), the calibration curves have been obtained by applying relatively low constant potential of 200 mV (vs. SCE). The NPG/PEDOT/GOx (2CVs) biosensor exhibits high sensitivity of 7.3 μA mM^{-1} cm^{-2} and a wide linear range of 0.1–15 mM, making it suitable for reliable analytic applications.

© 2013 Elsevier B.V. All rights reserved.

1. Introduction

Development of amperometric glucose biosensors is currently one of the most active areas of interests concerning research. The determination of glucose in the blood plays a crucial role in aspects for food safety and health, especially for diabetes [1]. To fabricate novel biosensors, many immobilization strategies have been adopted such as covalent binding, cross-linking, adsorption and entrapment [2]. Conducting polymers (CPs), which are high conductive, superiorly stable, easily synthesized and suitable for electrochemical reactions, have been used for enzyme immobilization [3]. The entrapment of enzyme molecules within CP film by polymerizing the monomers in the presence of enzyme is a fast and attractive approach to construct biosensors. In addition, the thickness of sensing film can be easily controlled by changing the number of cycles or deposition time during electropolymerization [4].

Among the promising family of CPs, poly(3,4-ethylenedioxythiophene) (PEDOT) can serve as electrochemically stable, homogeneous and versatile films [5]. Additionally, 3,4-ethylenedioxythiophene (EDOT), is commercially available and can be facilely electropolymerized at relatively low applied potentials even in aqueous solutions [6,7]. Since Fabiano and his coworkers firstly found the GOx entrapment in PEDOT on the surface of Pt disks [8], there are continuing interests for development of new materials to improve sensor behaviors dependent on biocompatibility for enzyme and enhancement of electron transfer. In recent years, graphene/PEDOT [9] and PEDOT/Au nanoparticles [10] have been developed for biosensor applications due to their unique properties. However, graphene would have a big risk for in-vivo detection taking its nano-toxicity into account [11], and Au nanoparticles need the substrate for support [12], which have shown limitation in practical applications like online medical monitoring.

Dealloyed nanoporous gold (NPG) is a new and developing material, which possesses self-organized and three-dimensional nanoporous structure in a self-supporting bulk form [13]. NPG has attracted tremendous attentions as widely used multifunctional materials in electroanalysis [14,15], energy storage [16,17], biofuel cells [18], and catalysis [19,20]. In addition, the ultrathin hybrid films of NPG and CPs, such as NPG/polypyrole [21] and NPG/polyaniline [22], have been achieved as high-performance electrochemical supercapacitors due to their promising electron transfer capability, "soft" mechanical property and high stability. Meanwhile, NPG is biocompatible for enzyme immobilization [23]. It is thereby expected that NPG/CPs composites will show synergistic effects in the electrochemical performance, considering their superiorities, specific nanostructure, good interaction, ultrathin and flexible membrane. In this study, we firstly report a one-step fabricated NPG/PEDOT/GOx hybrid electrodes that would shine the way to explore novel biosensors in future.

* Corresponding author. Tel.: +865 318 839 9858.
E-mail address: pcsi@sdu.edu.cn (P. Si).

0039-9140/$ - see front matter © 2013 Elsevier B.V. All rights reserved.
http://dx.doi.org/10.1016/j.talanta.2013.08.014

2. Experiment section

2.1. Reagents and apparatus

GOx from *Aspergillus niger* (EC 1.1.3.4, type II, ≥15,000 units/g) was purchased from Sigma-Aldrich company (Saint Louis, USA). Sodium dihydrogen phosphate (AR grade), disodium hydrogen phosphate (AR grade), lithium perchlorate (99.9% metals basis), BQ, and β-D-glucose (GC, ≥99.5%) were supplied by Aladdin (China). EDOT, polyethylene glycol 20000 (PEG20000), sulfuric acid and nitric acid were ordered from Shanghai Sinopharm Chemical Co., Ltd. (Shanghai, China). All chemicals were used as received without any further purification.

All the electrochemical experiments were performed on a LK2005A electrochemical workstation system (Lanlike Company, Tianjin).A conventional three-electrode cell, which consisted of a working electrode of the enzyme modified NPG, a Pt wire counter electrode, and a reference electrode of saturated calomel electrode (SCE) or Ag/AgCl wire, was set up in this work. All potentials are reported with respect to SCE. Prior to electrochemical experiments, 20 min nitrogen bubbling was used to remove oxygen from all aqueous solutions.

Morphology characterization of NPG and NPG/PEDOT/GOx samples was performed by field emission scanning electron microscope (FESEM, Hitachi SU-70) and transmission electron microscopy (TEM, JEOL JEM-2100).

Fourier-transform infrared (FTIR) spectra were collected using a Bruker Tensor-37 series FTIR spectrophotometer with samples prepared as KBr pellets.

2.2. Preparation of NPG electrodes

Dealloyed NPG sheets were prepared by floating 100-nm-thick Au/Ag leaves (12-carat, Sepp Leaf Products, New York) in concentrated HNO_3 for 30 min at 30 °C. After carefully cleaned with ultrapure water, the free-standing NPG films were placed on the pre-polished mirror like surface of glassy carbon electrode (GCE) with a diameter of 4 mm, and stored in a desiccator before next using.

2.3. Preparation of the enzyme electrode

The fabrication strategy of NPG/PEDOT/GOx has been described in Fig. 1A. Briefly, enzyme entrapment was performed by scanning the potential from 200 mV to 1300 mV (vs. Ag/AgCl) at 100 mV s^{-1}. And different scan cycles were utilized to synthesize a series of enzyme electrodes with various polymer thicknesses. The electropolymerization solution consisted of 40 mg ml^{-1} GOx, 20 mM EDOT, 1 mM PEG, 0.1 M pH 7.0 phosphate buffer solution (PBS) and 0.1 M $LiClO_4$. Same procedure was also used to fabricate planar polycrystalline gold (polyAu) based enzyme electrodes, denoted as Au/PEDOT/GOx. The resulted electrodes were stored in 0.1 M pH 7.0 PBS at 4 °C.

2.4. Electrochemical measurements

Cyclic voltammetry (CV) and single potential step chronoamperometry (SPSC) were performed in a 0.1 M pH 7.0 PBS containing 1 mM BQ, with a SCE reference electrode. Amperometric measurements of glucose were recorded under constant potentials with successive additions of 0.02 ml stock glucose solution (0.5 M).

3. Results and discussion

3.1. Electropolymerization

The solubility of EDOT in water is small (with a limit of ~14 mM at 20 °C) [24]. PEG is introduced to help EDOT to disperse well in aqueous solutions. The enhanced solubility of EDOT is the result of the formation of a pseudo–complex [25]. The electropolymerization process is shown in Fig. 1. Compared with the absence of enzyme (Fig. 1C), the lower peak current is observed in the presence of GOx (Fig. 1B), which is due to the incorporation of GOx with the PEDOT matrix. Since GOx from *Aspergillus niger* has an isoelectric point of 4.2 [26], it is supposed that negatively charged enzyme molecules can serve as the counter-ions during immobilization procedure (pH 7.0) rather than physical entrapment alone [27].

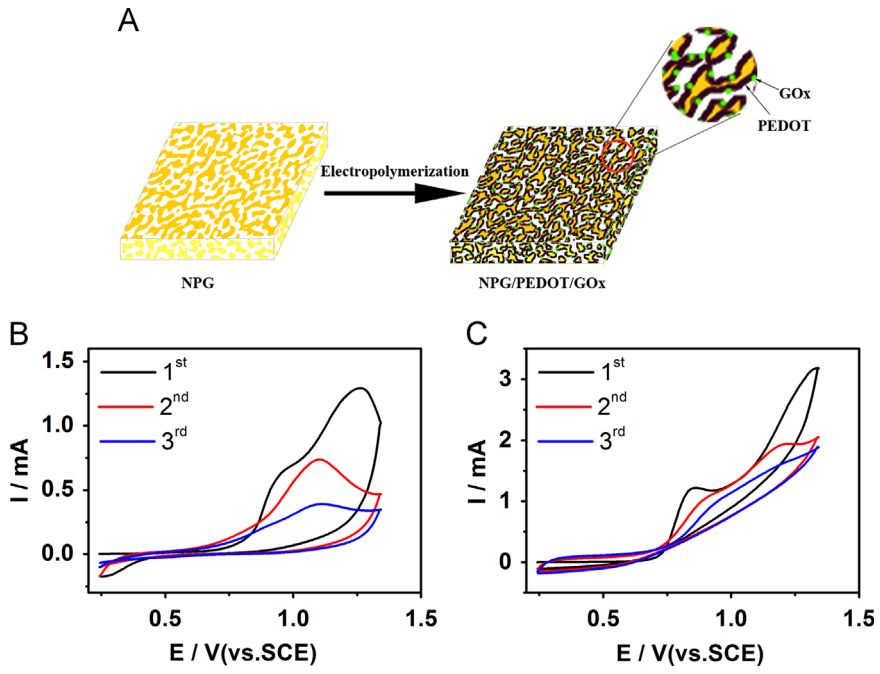

Fig. 1. Schematic drawing of the electropolymerization of NPG/PEDOT/GOx (A), Cyclic voltammograms of 20 mM EDOT in 0.1 M PBS (pH 7.0) containing 1 mM PEG, 0.1 M $LiClO_4$ with (B) and without (C) 40 mg ml^{-1} GOx present: NPG working electrode; scan rate, 100 mV s^{-1}.

The cyclic voltammograms (Fig. 1B) show the irreversible anodic curves, which reveal the formation of the conducting polymer. The onset of the anodic current appears at about 700 mV (vs. SCE). In the range of higher applied potential, two anodic peaks can be seen in the first cycle. The first peak (at around 900 mV) is attributed to the adsorption of oxidized EDOT onto the electrode, while the second peak (at around 1.25 V) is caused by the oxidation of EDOT diffusing close to the electrode [25]. The anodic currents decrease in the 2nd and 3rd sweeps and only one broad peak appears, which is probably due to the growth of oxidized EDOT [5]. Compared with the normal gold electrodes (data not shown), the cycles of electropolymerization performed on NPG electrodes show the lower onset potential and higher intensity of anodic peaks. It is inferred that the high conductivity and high active surface area of NPG can facilitate the electron transfer and improve the performance of the polymer films [21].

Generally, an ideal biosensor will have a thin sensing layer for a fast response, and its biochemical activity relates to the amount of selective molecules in the layer [29]. In this way, it is supposed that more cycles during the electrodeposition would lead to a thicker NPG/PEDOT/GOx nanocomposite membrane and more GOx molecules would be entrapped. Fig. 2B shows dependence of CVs in the electropolymerization process on NPG/PEDOT/GOx electrodes response to glucose. However, unlike 15 cycles for the planar platinum electrode [8], only two cycles' manner is found to be appropriate for sufficient enzyme loading and effective substrate diffusing, which is in agreement with Randles-Sevcik relationship [30]. As shown in Fig. 2A, the decreasing slope with increased cycles means the worse mass transport and the greater resistance for chemicals diffusion through the conducting polymeric matrix. In this work, optimal number of scanning cycles is 2 to obtain the highest sensitivity.

3.2. Optimization of the film thickness

NPG shows high electroactivity towards the redox process of BQ. It is observed Au/PEDOT/GOx (2CVs) exhibits an anodic peak at 320 mV (vs. SCE) at the scan rate of 50 mV s^{-1} (Fig. 2A), while the NPG/PEDOT/GOx (2CVs) displays the anodic peak at 145 mV (Fig. 2B). The obvious peak shift perhaps attributes to the existence of specific crystalline planes of NPG, which has also been confirmed by spherical aberration-corrected TEM [13]. Meanwhile, the redox reaction of BQ belongs to inner-sphere mechanism, which strongly depends on the surface conditions [28]. The active surface of NPG will thereby give more remarkable effect on the inner-sphere reaction compared with that on the normal planar ployAu. Fully understanding of the electron transfer inside NPG will be proposed in our coming research report. Fig. 2A shows linear relationships between the oxidation peak currents of BQ and square root of scan rates at different enzyme modified electrodes with various film thicknesses, indicating the diffusion controlled reaction for free BQ.

3.3. Morphology characterization and FTIR analysis

The nanostructure morphologies of the bare NPG and optimized NPG/PEDOT/GOx (2CVs) have been confirmed by SEM (Fig. 3A and B). The SEM images of the active NPG display the bicontinuous nanoporous structure, with a homogeneous pore/ligament size of ~30 nm. After the electrodeposition of PEDOT on NPG electrodes, the pores become smaller and the ligaments grow thicker, the nanoporous structure indeed preserve. EDX spectra also help us to make sure the formation of PEDOT, with the existence of elements *N* and *S* (Fig. 3E and F). The PEDOT has been uniformly grown on the surfaces of NPG ligaments with intimate interaction between PEDOT and NPG as shown in TEM images (Fig. 3C and D). The PEDOT film is as thin as around 10 nm (Fig. 3D), which would cause a fast response during the biosensing work [31]. In the light of ultrathin NPG/PEDOT hybrid film, it allows miniature biosensors fabricated in a facile way.

As shown in Fig. S3, there are no obvious differences between the FTIR spectra of NPG/PEDOT and NPG/PEDOT/GOx hybrid.

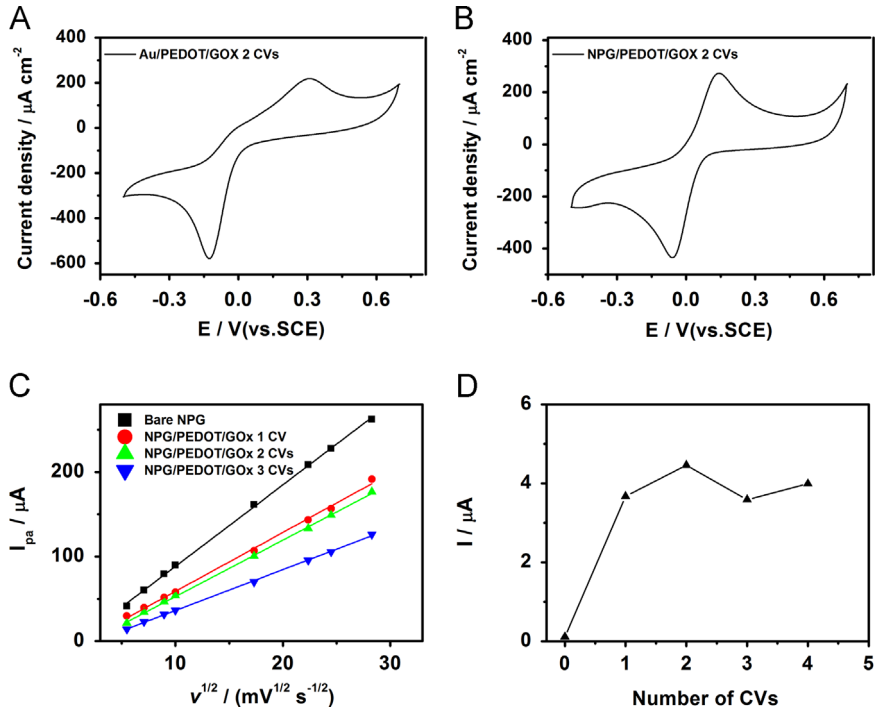

Fig. 2. CVs of Au/PEDOT/GOx (2CVs) (A) and NPG/PEDOT/GOx (2CVs) (B) in 0.1 M pH 7.0 PBS containing of 1 mM BQ; scan rates 50 mV s^{-1}; Calibration plots of the oxidation peak current vs. square root of scan rate obtained by CV in 1 mM BQ (pH 7.0 PBS) various scan rates (mV s^{-1}): 30, 50, 80, 100, 300, 500, 600, 800 (C); Effect of number of CVs on NPG/PEDOT/GOx electrodes response to glucose. Conditions: 5 mM glucose, 1 mM BQ in 0.1 M pH 7.0 PBS, 200 mV vs. SCE (D).

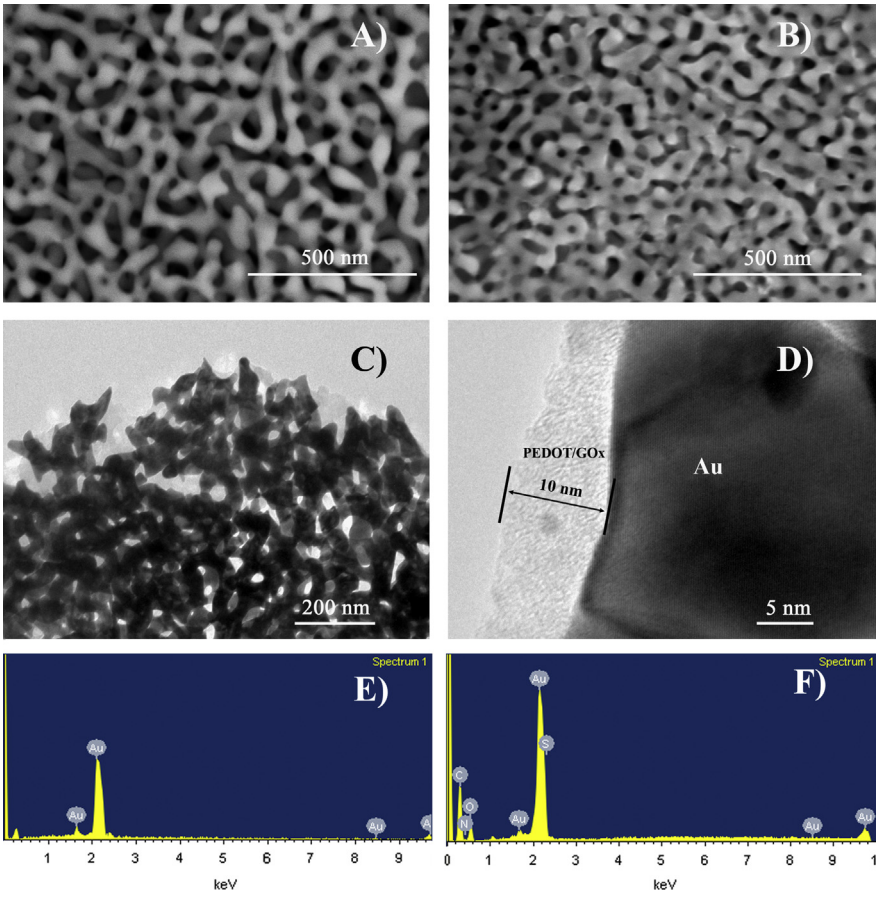

Fig. 3. SEM images of NPG (A) and NPG/PEDOT/GOx (2CVs) (B). TEM images of NPG/PEDOT/GOx (2CVs) (C, D). (EDX) spectra of bare NPG (E) and NPG/PEDOT/GOx(2 CVs) (F).

The bands in the range of 600–800 cm^{-1} assign to the fingerprint absorption of PEDOT. The main bands are situated at 1087 cm-1 (C–O–C bond stretching), 1261 cm^{-1} (the coupling of C–O–C stretching and CH deformation modes), 1323 and 1393 cm^{-1} (*C*═*C* in-plane ring vibrations). Therefore, PEDOT is successfully electropolymerized in this work.

3.4. *Response to glucose*

The classical amperometric curves of the biosensors are recorded by successively adding 1 mM glucose at constant potentials (Fig. 4A and B). Inspired from the CV results (Fig. 2A and B), the detection potentials for NPG and normal polyAu based biosensors are 200 mV and 400 mV, respectively. It is predicted that the lower applied potential for NPG modified biosensor would be beneficial to extend their lifetime and avoid the interference from commonly coexisted ascorbic acid or uric acid in the real samples. With increasing glucose concentration, the amperometric response of the optimized NPG/PEDOT/GOx (2CVs) is increased. The current responds to the substrate quickly and the detection curves reach a plateau (90% steady state [32]) in 15 s.

Fig. 4C displays the calibration curves. The NPG based biosensor exhibits a linear range of 0.1–15 mM with a correlation coefficient of 0.99824. This linear range is wider than the realm of blood glucose concentration in human body (i.e 2–10 mM) [33] and some other previously reported glucose biosensors based on CP entrapment [8–34]. The sensitivity obtained from the linear segment of the calibration is 7.3 μA mM^{-1} cm^{-2}, which is comparable with similar biosensors (Table. S3). And the main feature for the strategy is that NPG/PEDOT based biosensor with an ultrathin selective film (around 10 nm) can be fabricated by a robust electrochemical method. The limit of detection (LOD) is estimated to be 10 μM at a signal-to-noise ratio of 3. While for the normal polyAu based biosensor, the sensitivity and the upper limit of linear range are 2.3 μA mM^{-1} cm^{-2} and 9 mM (with a correlation coefficient of 0.98991), separately. Compared with the normal polyAu, NPG based biosensor has the improved response to glucose probably due to its high specific active area and fixed adhesion of GOx within the polymeric matrix. The unique nanoporous structure with highly active surface will enhance biomolecules immobilization into polymer film, increase enzyme loading and accelerate electron transfer of mediators. In addition, the robust immobilization will keep bioactivity of enzyme and improve affinity of enzyme to substrate [35].

One specific enzyme electrode for eight continuous determinations shows a relative standard deviation (R.S.D.) of 3.79% in the presence of 3 mM glucose (Table. S1). The reproducibility of the sensors constructed by the same procedure is evaluated by independent measurements for the amperometric response to 3 mM glucose, providing a R.S.D. of 5.59% (Table. S2.). The selectivity of the resulted electrode to glucose is evaluated in the presence of 0.1 mM ascorbic acid (AA) and 0.1 mM uric acid (UA) in a 0.1 M PBS solution (pH 7.4) containing 1 mM BQ. Compared with the response to 3 mM glucose, it can be seen from the Fig. S5 the selectivity of NPG/PEDOT/GOx electrode sensor is very good in detecting glucose in its normal physiological level in the presence of 0.1 mM AA and 0.1 mM UA.

Long term stability is a crucial parameter of biosensors [32], which has been evaluated here by monitoring the current response for 5 mM glucose each day. After 7 days, the sensor can retain above 85% of its original current response (Fig. 4D). In our study, there are several crucial factors influencing the stability:

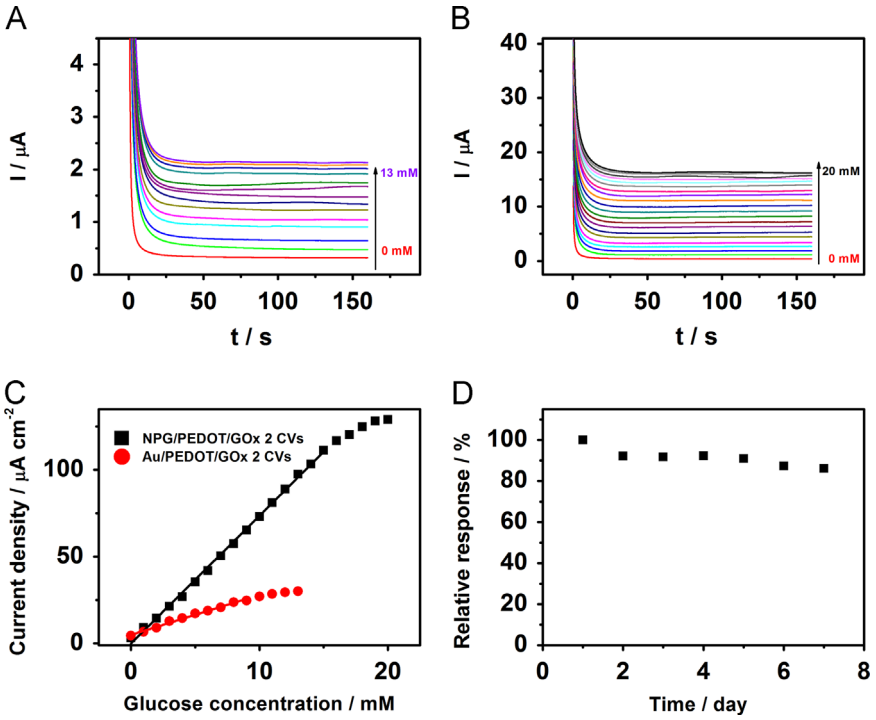

Fig. 4. Current-time plots of Au/PEDOT/GOx (2CVs) (A) and NPG/PEDOT/GOx (2CVs) (B) with various glucose concentrations at detection potentials (200 mV and 400 mV vs. SCE, respectively). The electrolyte contains 0.1 M pH 7.0 PBS and 1 mM BQ; (C) Calibration plot of NPG/PEDOT/GOx (2CVs) and Au/PEDOT/GOx (2CVs). Solid lines demonstrate the linear range; (D) Long term stability of NPG/PEDOT/GOx (2CVs). Conditions: 5 mM glucose in 0.1 M pH 7.0 PBS, 200 mV vs. SCE.

firstly, PEDOT possess high inherent stability in an aqueous environment [36]; secondly, NPG/PEDOT is tightly adhesive, as a robust matrix for enzyme loading; thirdly, NPG provides confined 3D nanoporous structure for the detection potential as low as 200 mV (vs. SCE); and fourthly, free BQ used as the mediator, instead of O_2, will avoid the damage from hydrogen peroxide [3].

4. Conclusions

In the present work, NPG/PEDOT/GOx hybrid films have been synthesized by one-step electropolymerization. Under the relatively low constant potential of 200 mV (vs. SCE) and mediated by BQ, the biosensors are selectively response to glucose. We have demonstrated the truly support-free NPG is suitable for enzyme immobilization, due to its high surface-to-volume ratio, electrocatalytic activity and biocompatibility. Additionally, the performance of glucose determination depends on the thickness of the biocomposite film. The optimized NPG/PEDOT/GOx biosensor prepared by only two cycles is appropriate for sufficient enzyme loading and effective substrate diffusing, which exhibits comparable sensor performance, with wide linear range (0.1–15 mM) and high sensitivity (7.3 μA mM^{-1} cm^{-2}). The proposed NPG/CP based biosensor construction strategy is expected to extend to other redox enzymes. We believe that this convenient, low-cost and scalable NPG/CP film will be an ideal candidate for biosensor and biofuel cell applications.

Acknowledgments

This work was sponsored by the National 973 (2012CB932800) Program Project of China. We also thank the support from the Shandong University (No. 31370056431211 and no. 31370070-614018). We appreciate the kind support and meaningful discussion with Prof. Yi Ding and his group members.

Appendix A. Supporting information

Supplementary data associated with this article can be found in the online version at http://dx.doi.org/10.1016/j.talanta.2013.08.014.

References

[1] J. Wang, Analytical electrochemistry, 2nd ed., Wiley, New York, 2000.
[2] J.H.T. Luong, A. Mulchandani, G.G. Guilbault, Trends. Biotechnol. 6 (1988) 310–316.
[3] T. Ahuja, I.A. Mir, D. Kumar, Rajesh, Biomaterials 28 (2007) 791–805.
[4] B.D. Malhotra, A. Chaubey, S.P. Singh, Anal. Chim. Acta. 578 (2006) 59–74.
[5] H. Yamato, M. Ohwa, W. Wernet, J. Electroanal. Chem. 397 (1995) 163–170.
[6] A.H.L. Pigani, Á. Colina, R. Seeber, J. López-Palacios, Electrochem. Commun. 6 (2004) 1192–1198.
[7] G. Heywang, F. Jonas, Adv. Mater. 4 (1992) 116–118.
[8] S. Fabiano, C Tran-Minh, B. Piro, L.A. Dang, M.C. Pham, O. Vittori, Mater. Sci. Eng., C 21 (2002) 61–67.
[9] L.M. Lu, O. Zhang, J.K. Xu, Y.P. Wen, X.M. Duan, H.M. Yu, L.P. Wu, T. Nie, Sens. Actuators B: Chem. (2013) 567–574.
[10] J.J. Xu, R. Peng, Q. Ran, Y.Z. Xian, Y. Tian, L.T. Jin, Talanta 82 (2010) 1511–1515.
[11] X.Y. Zhang, J.L. Yin, C. Peng, W.Q. Hu, Z.Y. Zhu, W.X. Li, C.H. Fan, Q. Huang, Carbon 49 (2011) 986–995.
[12] M. Tominaga, T. Shimazoe, M. Nagashima, I. Taniguchi, Electrochem. Commun. 7 (2005) 189–193.
[13] T. Fujita, P.F. Guan, K. McKenna, X.Y. Lang, A. Hirata, L. Zhang, T. Tokunaga, S. Arai, Y. Yamamoto, N. Tanaka, Y. Ishikawa, N. Asao, Y. Yamamoto, J. Erlebacher, M.W. Chen, Nat. Mater. 11 (2012) 775–780.
[14] F.H. Meng, X.L. Yan, J.G. Liu, J. Gu, Z.G. Zou, Electrochim. Acta 56 (2011) 4657–4662.
[15] Z.N. Liu, J.G. Du, C.C. Qiu, L.H. Huang, H.Y. Ma, D.Z. Shen, Y. Ding, Electrochem. Commun. 11 (2009) 1365–1368.
[16] Y. Yu, L. Gu, X.Y. Lang, C.B. Zhu, T. Fujita, M.W. Chen, J. Maier, Adv. Mater. 23 (2011) 2443–2447.
[17] X.Y. Lang, A. Hirata, T. Fujita, M.W. Chen, Nat. Nanotechnol. 6 (2011) 232–236.
[18] M. Hakamada, M. Takahashi, M. Mabuchi, Gold Bull. 45 (2011) 9–15.
[19] R. Zeis, T. Lei, K. Sieradzki, J. Snyder, J. Erlebacher, J. Catal. 253 (2008) 132–138.
[20] Y. Ding, M.W. Chen, MRS Bull. 34 (2009) 569–576.
[21] F.H. Meng, Y. Ding, Adv. Mater. 23 (2011) 4098–4102.
[22] X.Y. Lang, L. Zhang, T. Fujita, Y. Ding, M.W. Chen, J. Power Sources 197 (2012) 325–329.
[23] X. Wang, X.Y. Liu, X.L. Yan, P. Zhao, Y. Ding, P. Xu, PLoS ONE 6 (2011).
[24] Y. Kudoh, K. Akami, Y. Matsuya, Synth. Met. 98 (1998) 65–70.

[25] N. Sakmeche, S. Aeiyach, J.J. Aaron, M. Jouini, J.C. Lacroix, P.C. Lacaze, Langmuir 15 (1999) 2566–2574.
[26] J.H. Pazur, K. Kleppe, Biochemistry 3 (1964) 578–583.
[27] S.B. Adeloju, Al.N. Moline, Biosens. Bioelectron. 16 (2001) 133–139.
[28] S.H. DuVall, R.L. McCreery, Anal. Chem. 71 (1999) 4594–4602.
[29] P.N. Bartlett, R.G. Whitaker, J. Electroanal. Chem. 224 (1987) 27–35.
[30] A.J. Bard, L.R. Faulkner, ELECTROCHEMICAL METHODS Fundamentals and applications, John Wiley & Sons Inc., New York (2001), (2001).
[31] X.L. Luo, J.J. Xu, Y. Du, H.Y. Chen, Anal. Biochem. 334 (2004) 284–289.
[32] D.R. Thévenota, K. Tothb, R.A. Durstc, G.S. Wilsond, Biosens. Bioelectron. 16 (2001) 121–131.
[33] K.E. Toghill, R.G. Compton, Int. J. Electrochem. Sci. 5 (2010) 1246–1301.
[34] N.C. Foulds, C.R. Lowe, J. Chem. Soc., Faraday Trans. 1 (82) (1986) 1259–1264.
[35] L.Y. Chen, T. Fujita, M.W. Chen, Electrochim. Acta. 67 (2012) 1–5.
[36] A. Krosa, N.A.J.M. Sommerdijk, R.J.M. Nolte, Sens Actuators B: Chem. 106 (2005) 289–295.